CO$_2$ and CH$_4$ exchanges between moist moss tundra and atmosphere on Kapp Linne, Svalbard

Anders Lindroth[1], Norbert Pirk[2], Ingibjörg S Jónsdóttir[3], Christian Stiegler[4], Leif Klemedtsson[5], and Mats B Nilsson[6]

[1]Department of Physical Geography and Ecosystem Science, Lund University, Lund, Sweden.

[2]Department of Geosciences, University of Oslo, Oslo, Norway.

[3]Life and Environmental Sciences, University of Iceland, Reykjavik, Iceland.

[4]Bioclimatology, Georg-August Universität Göttingen, Göttingen, Germany.

[5]Department of Earth Sciences, University of Gothenburg, Gothenburg, Sweden.

[6]Department of Forest Ecology and Management, Swedish University of Agricultural Sciences, Umeå, Sweden.

Corresponding author: anders.lindroth@nateko.lu.se

Abstract

We measured CO_2 and CH_4 fluxes using chambers and eddy covariance (only CO_2) from a moist moss tundra in Svalbard. The average net ecosystem exchange (NEE) during the summer (9 June-31 August) was negative (sink) with -0.139 ± 0.032 µmol m^{-2}s^{-1} corresponding to -11.8 g C m^{-2} for the whole summer. The cumulated NEE over the whole growing season (day no. 160 to 284) was -2.5 g C m^{-2}. The CH_4 flux during the summer period showed a large spatial and temporal variability. The mean value of all 214 samples was 0.000511 ± 0.000315 µmol m^{-2}s^{-1} which corresponds to a growing season estimate of 0.04 to 0.16 g CH_4 m^{-2}. Thus, we find that this moss tundra ecosystem is closely in balance with the atmosphere during growing season when regarding exchanges of CO_2 and CH_4. The sink of CO_2 as well as the source of CH_4 are small in comparison with other tundra ecosystems in high Arctic.

Air temperature, soil moisture and greenness index contributed significantly to explain the variation in ecosystem respiration (R_{eco}) while active layer depth, soil moisture and greenness index were the variables that best explained CH_4 emissions. Estimate of temperature sensitivity of R_{eco} and gross primary productivity (GPP) showed that the sensitivity is slightly higher for GPP than for R_{eco} in the interval $0 – 4.5$ ºC, thereafter the difference is small up to about 6 ºC and then it began to raise rapidly for R_{eco}. The consequence of this, for a small increase in air temperature of 1 degree (all other variables assumed unchanged) was that the respiration increased more than photosynthesis turning the small sink into a small source (4.5 gC m^{-2}) during the growing season. Thus, we cannot rule out that the reason why the moss tundra is close to balance today is an effect of the warming that has already taken place in Svalbard.

1 Introduction

Climate warming is predicted to be most evident at high latitudes (Friedlingstein et al., 2006) with profound effects on ecosystem functioning. One of the high latitude regions that are expected to experience the most dramatic changes caused by climate change is the Arctic. This region which is located roughly north of the tree-line is characterized by cold winters and cool summers and with mean annual temperatures below zero. The summer periods are short ranging between 3.5 to 1.5 months from the southern boundary to the north and July is normally the warmest month. Annual precipitation is generally low decreasing from about 250 mm in the southern areas to 45 mm in polar deserts in the north (Callaghan et al., 2005).

The permafrost soils in the Arctic store 1035 ± 150 Pg of organic carbon in the top 0-3 m (Hugelius et al., 2014) which is more than the average 2010-2019 of 860 Pg of carbon in the atmosphere (Friedlingstein et al., 2020). The increased warming in these areas can induce higher decomposition rates due to increased microbial activity which will provide a positive feedback to the climate system (Schuur et al., 2015). On the other hand, warming can also increase photosynthesis and carbon uptake and thus compensate for, or exceed, the effect of increased decomposition. Climate warming is also affecting plant community composition and the length of the growing season (Post et al., 2009) which also has an impact on the processes regulating annual carbon emissions and uptake (Bosiö et al., 2014). There is however a large uncertainty regarding the timing, magnitude and possible sign of potential feedbacks caused by these changes (Myers-Smith et al., 2020).

Understanding processes that are controlling the exchanges of greenhouse gases in the Arctic is crucial for assessment of potential feedback effects. For this purpose, multiple year-around long-term studies including direct measurements of CO_2 and CH_4 fluxes covering all seasons, winter, spring, summer and autumn would be ideal. This is a great challenge in the harsh climate of the Arctic and with limited support of key infrastructures for, e.g., provision of electricity for operation of instruments.

In spite of these difficulties a few year-around studies have been performed during the last couple of decades. In the low Arctic, Oechel et al. (2013) demonstrate the importance of the wintertime fluxes in a tussock tundra ecosystem in Alaska. They found that the non-summer season emitted more CO_2 than the corresponding uptake during the summer resulting in a net source to the atmosphere of about 14 g C m^{-2} on an annual basis. They also showed that the shoulder seasons, spring and autumn roughly out-weighted the summer uptake. Euskirchen et al. (2012, 2016) measured net CO_2 exchange in three different tundra ecosystems; heath tundra, tussock tundra and wet sedge tundra in northern Alaska over three years. They found that the uptake of -51 to -95 g C m^{-2} during the summer (June-August) was overturned by the respiration that occurred during the winter period resulting in net annual losses for all three ecosystems. Zhang et al. (2019) reported five years of year-around flux measurements in a heath ecosystem on west Greenland and they found that the heath was an annual sink of -35±15 g C m^{-2}. One year with an anomalously deep snow pack showed a 3-fold higher respiration during the winter as compared to the other years which resulted in a significantly lower net uptake during that year.

Even fewer studies have been done on year-roud studies in the high Arctic. Lüers et al. (2014) quantified the annual CO_2 budget using eddy covariance measurements in a river catchment area near Ny-Ålesund on Spitsbergen in the Svalbard archipelago and they found that the ecosystem was in C-balance. The footprint area was a semi-polar desert with only 60% vegetation cover and patches of bare soil and stones. Also in Svalbard but further south in Adventdalen on a flat alluvial fen irregularly covered with ice wedged polygons, Pirk et al. (2017) made year-around measurements of CO_2 fluxes and found it to be a net sink of -82 g C m^{-2}. Because of the irregularities caused by the ice wedges and the differences in wetness, they focused the analyses on the spatial variability in two different directions, one wetter and one drier, and they estimated the annual net ecosystem exchange to -91 g C m^{-2} and -62 g C m^{-2} for the respective areas.

The Arctic ecosystems constitute also a source of CH_4 to the atmosphere even if it is not a very large one. Saunois et al. (2020) estimated that the Northern high latitude region (60ºN - 90ºN) contributed 4% of global emissions and emissions from wetlands are only part of the emissions from this region. However, in the light of the vulnerability of the high Arctic permafrost areas and considering the large carbon pool and the predicted changes in climate, a quantification and understanding of CH_4 exchanges in these areas are still important. Christensen et al. (2004) showed one example of a dramatic impact of the climate warming on the CH_4 emissions in a permafrost mire in sub-arctic Sweden. The warming which is visible in this area since decades and its impact on permafrost and vegetation changes was estimated to have caused an increase of landscape CH_4 emissions in the range 22-66% in the period 1970 to 2000.

Mastepanov et al. (2008) were the first to show the importance of emissions also outside of the growing season. They observed a large burst of CH_4 from a fen area in Zackenberg, Greenland

after the growing season and during the time when the soil started to freeze. This finding was confirmed in a later paper (Mastepanov et al., 2013) and the process was hypothetically attributed to the subsurface CH_4 pool. Hydrology and vegetation composition play an important role for CH_4 emission and dynamics. McGuire et al. (2012) made a comprehensive summary of CH_4 exchanges of the Arctic tundra showing the difference between wet and dry ecosystems; the wet tundra emitted 5.4 to 13.0 g CH_4-C m^{-2} during summer and 8.5 to 20.2 g CH_4-C m^{-2} annually. The corresponding values for the dry/mesic tundra were 0.3 to 1.4 g CH_4-C m^{-2} and 0.3 to 4.3 g CH_4-C m^{-2}, respectively. Bao et al. (2021) utilized year-around measurements of CH_4 fluxes from three sites of the Ameriflux network in Northern Alaska to demonstrate the importance of the spring and autumn seasons for the annual emission. The shoulder seasons contributed about 25% of the annual emissions and the autumn season had about three times higher emission than the spring season. These findings increasingly emphasise the importance of year-around measurements to fully understand the CH_4 controls and dynamics.

The main aim of this study is to provide another piece of the puzzle concerning CO_2 and CH_4 exchanges from different but widespread ecosystem types in the high Arctic. We hypothesise that this moist tundra ecosystem is a net carbon sink during the growing season and that the summer emissions of methane will be at levels comparable with other methane emitting high Arctic ecosystems. We made flux measurements of CO_2 and CH_4 in an moist moss tundra ecosystem situated at Kapp Linne on the west coast of the Svalbard archipelago in 2015 and with an additional campaign in 2016. The measurements in 2015 were done using both eddy covariance system (CO_2) and chambers (CO_2 and CH_4) but only chambers in 2016. We quantify ecosystem respiration (R_{eco}), gross primary productivity (GPP) and net ecosystem exchange (NEE) during the growing season based on a combination of chamber end eddy covariance measurements. The CH_4 emission was only quantified for the summer season. We also analyze the environmental controls of the fluxes.

2 Materials and Methods

2.1 Research site and measurements

This study was performed in the Svalbard archipelago near the weather station Isfjord Radio (78°03′08″ N 13°36′04″ E, alt. 7 m) which is located right on the foreland of Kapp Linné on the island of Spitzbergen (Fig. S1). The tundra area where the measurements were performed is located about 1 km southeast of the station. The study area consists of moist moss tundra, a widespread ecosysetem in Svalbard (Vanderpuye et al., 2002; Ravolainin et al., 2020). The vegetation is characterised by the moss species *Tomentypnum nitens, Sanionia uncinata* and *Aulocomium palustre* and a sparse cover of vascular plants (20-40%), dominated by *Equisetum arvense, Salix polaris* and *Bistorta vivipara*. Other vascular plant species found in the plots: *Saxifraga cespitosa*, *Saxifraga oppositifolia*, *Silene aucaulis*, and some grass species, most likely *Alopecurus ovatus* (previously *A. borealis*), and *Poa arctica*. The vegetation analysis was made from photographs of chamber location plots taken between 26 June and 2 July 2015 (see Figs. S4a-4y in Supplement).

The net ecosystem exchange of CO_2 was measured with an eddy covariance (EC) system located centrally on the moss tundra (78°03′28.6″ N 13°38′40″ E). The sonic anemometer (USA-1;

Metek GmBH, Germany) was mounted on top of a tripod (see Fig. S1) at 2.7 m height. The CO_2 and H_2O concentrations were measured with an open path sensor (LI-7500; Li-Cor Inc., USA) placed just beneath the sonic and inclined about 30º pointing towards east. Radiation components, incoming and outgoing short-wave and long-wave (CNR-4; Kipp & Zonen, the Netherlands) were measured at 2.0 m height above ground with the sensor directed towards south. All sensors were connected to a datalogger (CR-1000; Campbell Scientific, USA) which was powered by a solar panel and a battery. The EC sensors were sampled and stored at 10 Hz and all other sensors were sampled at 0.1 Hz with storage of 30 min mean values. These measurements were made from 25 June to 17 September 2015. The total data coverage during this period was 47% with a longer break in the measurements between 28 July and 29 August. The impact of substantial gap filling of measured EC data and partial modelling in order to complete the full growing season is further discussed below.

The soil efflux of CO_2 and CH_4 was measured with a dark chamber connected to a gas analyzer (Ultraportable Greenhouse Gas Analyzer; Los Gatos Research, USA) on 24 locations within the EC average footprint area. A circular thin-steel frame, 15 cm in diameter and 15 cm high, was inserted ca 5 cm into the ground in each location. The sharp edge of the frames made it easy to insert them into the ground without damaging the vegetation and with minimal soil disturbance. A picture was taken of each frame (see Supplement) for documentation of vegetation and for calculation of different indexes. The chamber was also made from steel and it had a rubber seal in the end facing the frame (Fig. S2) to make it air tight when mounted on the frame. The volume of the chamber and the part of the frame raised above the surface was 5.3 L. A small fan was installed inside the chamber to provide good mixing of the air during measurement. A small weight (stone) was placed on top of the chamber during measurement to prevent it from moving due to wind gusts. During concentration measurement air was circulated in a closed loop between the chamber and the gas analyzer in ca. 10 m long 4 mm diameter polyethene tubes (see Fig. S2). The air flow through the analyzer was ca 1.2 L min^{-1}. The chamber was ventilated in the free air about 1 minute before each measurement which lasted for 5 minutes. The concentrations were recorded and stored once per second by the gas analyzer. The time stamp of the recorded data was used to identify measurement cycles for analysis of fluxes.

The chamber measurement positions were selected in the following way. The frames were grouped in two sections, one north-east and one south-west of the flux tower since it was expected that the main wind direction would be along that direction. Each group was then split into three subsections with four measurement points within each one of them. The locations were named S1:1-S1:4, S2:1-S2:4, S3:1-S3:4, N1:1-N1:4, N2:1-N2:4 and N3:1-SN3:4. The four measurement points within each subsection were then placed along a transect with 3-4 m between each point. This way it was possible to measure all four chamber locations without having to move the whole measurement system. Chamber measurements were made in three separate campaigns: mid-summer (26 June to 2 July 2015), late-summer (25-27 August 2015) and early-summer (14-15 June 2016). Each location was measured three times during each one of the three campaigns, a total of 216 measurements. Besides gas concentrations, also soil temperature (5 cm), soil moisture (0-5 cm) and active layer depth was measured during each campaign.

Meteorological data needed for analyses and gap-filling were obtained as follows: Hourly air temperature and relative humidity from Isfjord radio, half-hourly global radiation from Adventdalen, daily snow depth and ground ice conditions from Svalbard airport and monthly precipitation from Isfjord radio and Barentsburg. The distance between the measurement site and these stations are; Isfjord radio, 1 km, Barentsburg, 13 km, Svalbard airport, 46 km and Adventdalen, 50 km. Using data from the more distant locations, Svalbard airport and Adventdalen, introduces some additional uncertainty. Concerning global radiation data we could compare in situ measured half-hourly radiation with the corresponding data from Adventdalen for a shorter period and it showed general good agreement although with relatively large scatter ($y = 0.84x + 15.9$; $r^2=0.57$; n=580). According to Dobler et al. (2021) the amount of precipitation in the area where Kapp Linne and Svalbard airport are located don't show any significant differences on an annual basis. Vickers et al. (2020) analysed timing of snow cover in Svalbard and they show that the mean (2000-2019) first snow-free day is very similar in areas where Kapp Linne and Svalbard airport are located. Thus, we are confident that using data from these relatively remote locations does not introduce serious bias in our analyses. Data sources are given in Acknowledgement.

3. Data analysis

The rawdata from the eddy covariance flux measurements were analysed using the Eddypro software version 6.1.0 (Li-Cor, 2016). Correction was made for the impact of the additional heat flux in the sensor path of the open path analyzer on the flux calculations according Burba et al. (2008). Gap filling during the measurement period was made using the REddyProc online eddy covariance data processing tool developed at the Max Planck Institute for Biogeochemistry (Wutzler et al., 2018) without u* correction since we could not identify any threshold for u*. The u* threshold is generally low for low and smoth vegetation (Pastorello et al., 2020) and for a wind exposed site as ours, it is not surprising that such threshold could not be found. Flux partitioning was made with the daytime-based method according Lasslop et al. (2000). Only data of highest quality, i.e. class=0 was retained for the gap filling and further analyses. Gap filling outside of the EC measurement period to obtain the carbon balance for a full growing season was made by modeling using the Lloyd &Taylor (1994) model for for R_{eco} and an empirical light response function for GPP (see below). The measured respiration by chambers was used to obtain the parameters for R_{eco} and EC data was used for fitting of the light response function for GPP.

For flux footprint calculations the roughness length (z_0) is needed and it was calculated from the wind profile relationship in near neutral (-0.01<z/L<0.01) conditions:

$$z_0 = \frac{z_m}{e^{(u(z) \cdot \frac{k}{u^*})}}$$ (1)

where z_m is measurement height, $u(z)$ is wind speed at height z, k is von Karman's constant and u* is friction velocity. We used the flux footprint prediction (FFP) online tool by Kjun et al. (2015) to calculate the footprint climatology.

The fluxes from the chamber measurements were estimated from the time change of the concentrations using linear regression. Every individual measurement was inspected and

238 evaluated manually. These inspections showed that 50 seconds for CO_2 and 100 seconds for CH_4
239 were optimal to obtain near perfectly linear responses a few seconds after the chamber had been
240 placed on the frame. The slopes of the regressions were then used to calculate fluxes per unit
241 surface area. The flux detection limits for CO_2 and CH_4 were calculated in the following way:
242 first the peak-to peak variation in the respective gases were determined when the chamber was
243 ventilated in the free air and when conditions were steady. Then 20 sets of artificial 'fluxes' for
244 each gas species were estimated based on 100 randomly generated concentrations for each data
245 set. The peak-to-peak difference was used as seed (input) for the randomly generated values. The
246 95% value of the distribution of these randomly generated fluxes was taken as the flux detection
247 limit for the respective gas.

249 The pictures of the vegetation inside of the chamber frames were analysed using the ImageJ
250 (https://imagej.net) public domain software. The camera color channel information (digital
251 numbers for Red (R), Green (G) and Blue (B) channels) was collected from the JPEG pictures.
252 This type of pictures is for instance used in studies that are tracking the phenological
253 development of vegetation (e.g. Richardson et al., 2009). The so-called green index (GI) is
254 applied to detect differences in greenness of vegetation:

256 $GI = G/(R+G+B)$ (2)

258 This index was also estimated for the central footprint area (100 m radius) of the flux
259 measurement location using a picture taken at 160 m above the altitude of the measurement area.

260 Forward stepwise linear regression (Sigmaplot 12.5) was used to analyze the dependency of the
261 CO_2 and CH_4 fluxes on environmental variables. We tested for air temperature (T_a), soil moisture
262 (θ), soil temperature (T_s), active layer depth (ALD), measurement location (S_{id}) and GI.

264 For gap filling of R_{eco} we only had access to air temperature with full annual coverage and, thus,
265 we could only use this driver for estimation of the R_{eco}. The measured chamber CO_2 fluxes were
266 fitted to the Lloyd & Taylor (1994) model with air temperature (T_a) as independent variable:

268 $FCO_2 = a \cdot e^{b(\frac{1}{56.02} - \frac{1}{T_a+46.02})}$ (3)

270 During the EC measurement period (25 June to 17 September 2015) the GPP was estimated as:

272 $GPP = NEE_f - R_{eco}$ (4)

274 Where NEE_f is the gap filled NEE according to Wutzler et al. (2018). This way R_{eco} and GPP
275 become consistent with the measured and gap filled NEE. For the time before and after this
276 period NEE was estimated as the sum of modelled R_{eco} and modelled GPP. The data for the GPP
277 model was derived from:

279 $GPP_m = NEE_m - R_{eco}$ (5)

281 Where NEE_m is the measured net ecosystem exchange. The GPP_m was then fitted to a light
282 response function:

283
$$GPP_m = c1 + c2 \cdot c3/(c2 + R_g) \tag{6}$$

285

4 Results

287 For CO_2 exchanges and partitioning we combined the soil efflux measurements with the chamber
288 system with the eddy covariance flux measurements. This was crucial for the partitioning and for
289 gap filling because from 20 April to 20 August at this location the sun is above the horizon 24
290 hours of the day and this means that there were few occasions of dark nighttime measurements
291 with the eddy covariance system and all of these were collected at the very end of the summer.
292 We consider the chamber measurements that were distributed across the summer to be more
293 representative of R_{eco} for this location.

294

295 For CH_4 exchanges we don't have any eddy covariance measurements so we present only
296 chamber data for this variable.

297

298   4.1 Weather

299

300 The mean annual temperature at Kapp Linne was -1.5 ℃ during 2015 which was 3.5 ℃ higher
301 than the long-term mean (1961-1990) of -5.1 ℃. The summer (June-August) mean of 5.5 ℃ was
302 2.0 ℃ higher than the long-term mean for the same time period (Fig. 1). The summer
303 precipitation in 2015 was much lower, 58 mm as compared to the long-term precipitation which
304 was 121 mm. The annual precipitation was also lower, 431 mm compared to the long-term
305 precipitation which was 514 mm.
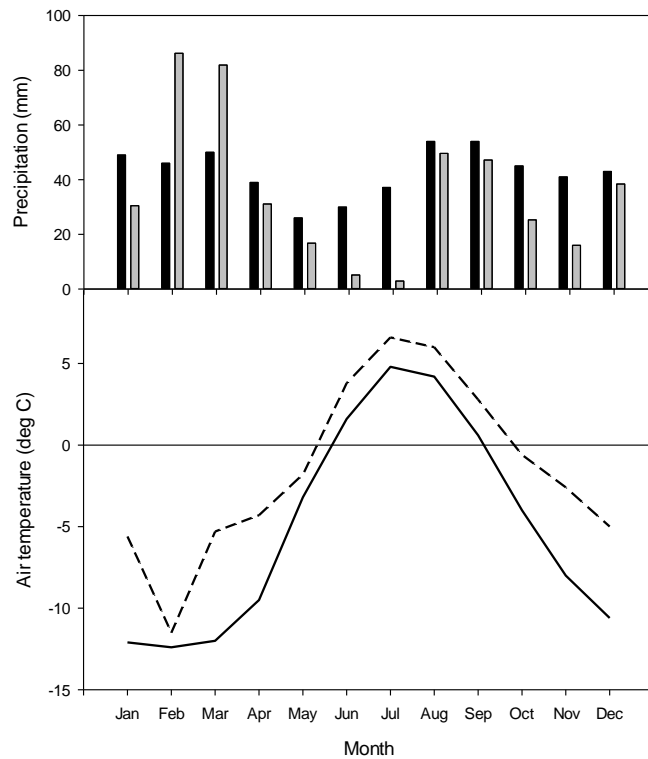
306
307 Figure 1. Monthly precipitation (top): Long-term average 1961-1990 black bars and 2015 grey
308 bars. Data from Barentsburg for January-May, from Isfjord Radio for June-December. Mean
309 monthly air temperature (bottom): Solid line is long-term average 1961-1990 and dotted line is
310 2015. Data from Isfjord Radio which is located about 1 km west of the investigation area.
311
312 We defined the growing season (the period during which vegetation is photosynthesizing) based
313 on the permanence of the snow pack which resulted in start day no. 160 and end day no. 284
314 (Fig. 2). The summer period which normally is defined as June through August was here defined
315 as lasting between 9 June (same as start of growing season) until end of August (Fig.2).
316
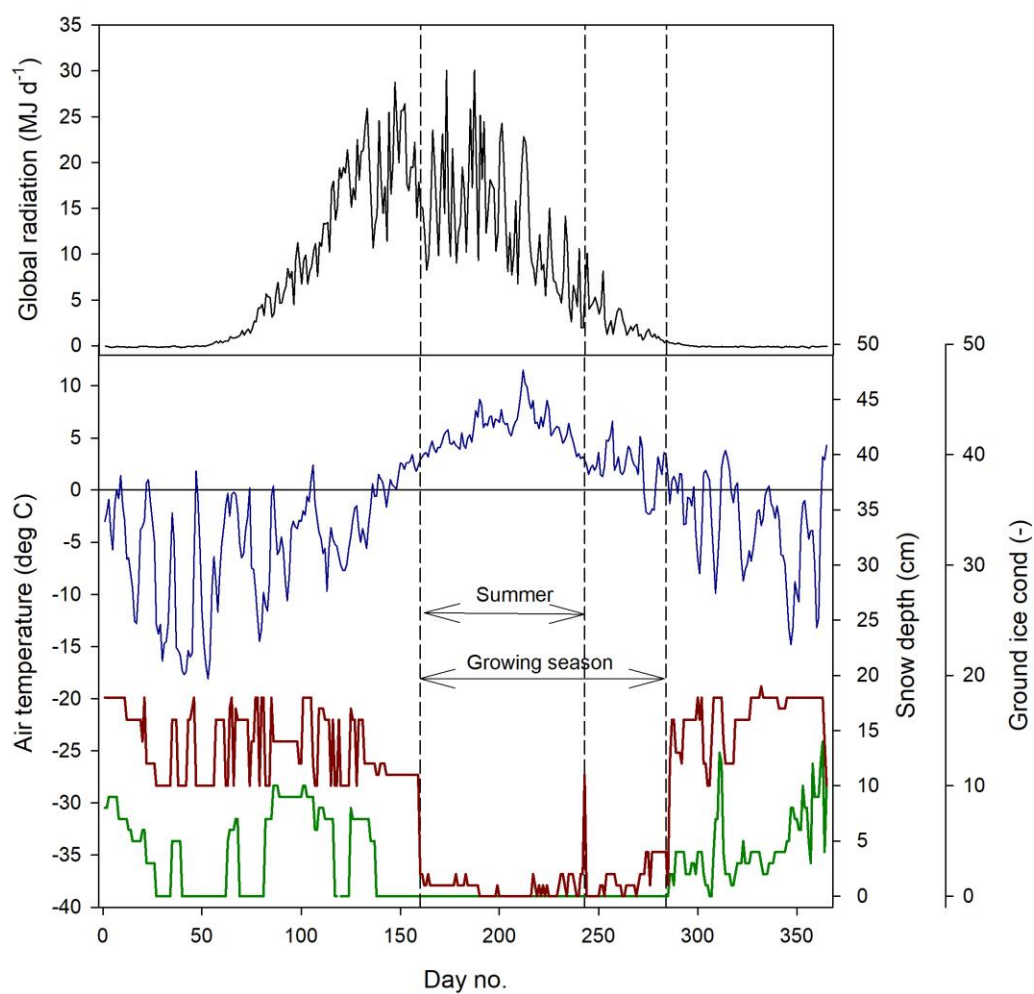
317
318
319 Figure 2. Weather conditions during 2015. Top panel: Mean daily global radiation at
320 Adventdalen. Bottom panel: Mean daily air temperature at Isfjord Radio (blue), snow depth (red)

321 and ground ice conditions (green) at Svalbard airport close to Longyearbyen. The ground ice
322 condition is scaled from 0 to 20 where 0 is no snow or ice on the ground and 20 indicate a
323 complete cover of snow or ice.
324
325   4.2 Flux footprint and greenness
326
327 The footprint climatology shows a good representativity of the moss tundra surface by the EC
328 measurements with 60-70% of fluxes emanating from areas well within the border of the tundra
329 (Fig. 3). The mean green index for a circular area with radius of 100 m centered at the flux tower
330 was 0.34 which corresponded exactly to the mean value for all chamber locations. The GI for the
331 24 chamber locations varied between 0.316 and 0.369. We observed a good (visual) correlation
332 between GI and coverage of green plants (see Figures S4a-S4y of chamber location pictures and
333 GI).
334
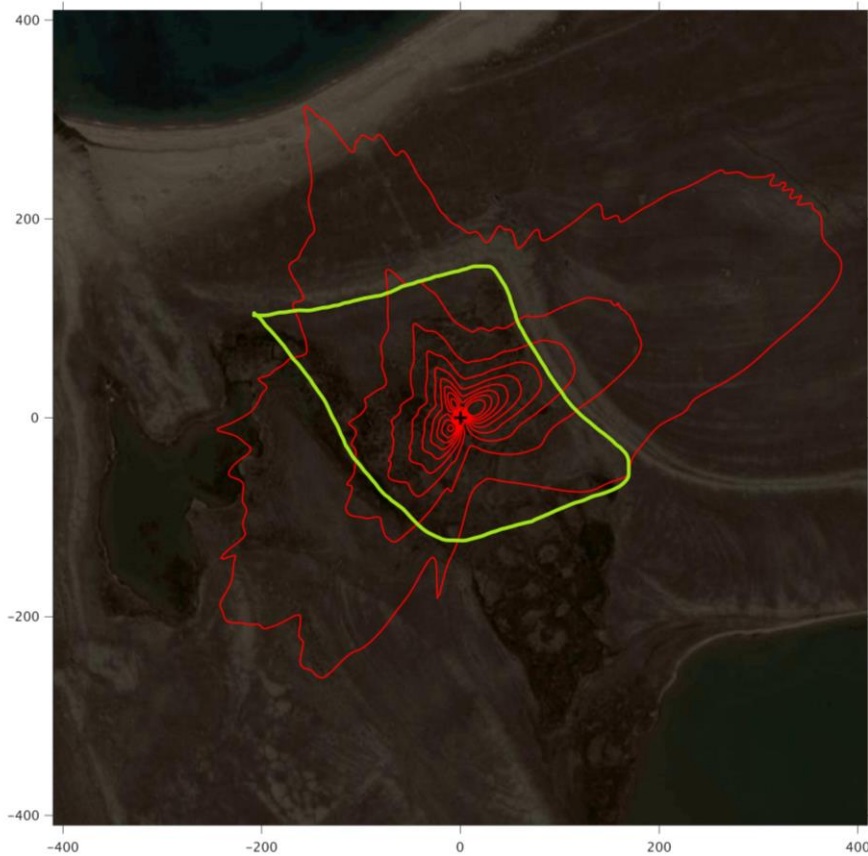
335
336 Figure 3. The footprint climatology with red contour lines 10-90%. The area within the green
337 line mark the heart of the moss tundra. The scale (m) is shown on the outer borders of the
338 picture.
339
340   4.3 CO$_2$ exchanges
341

342   The CO_2 fluxes from the chamber measurements showed quite large variation over time (Fig. 4)
343   and across sampling locations (Fig. 5). The mean CO_2 flux of all samples was 0.81±0.11 µmol
344    $m^{-2}s^{-1}$. The uncertainty is given as the 95 confidence limit.
345
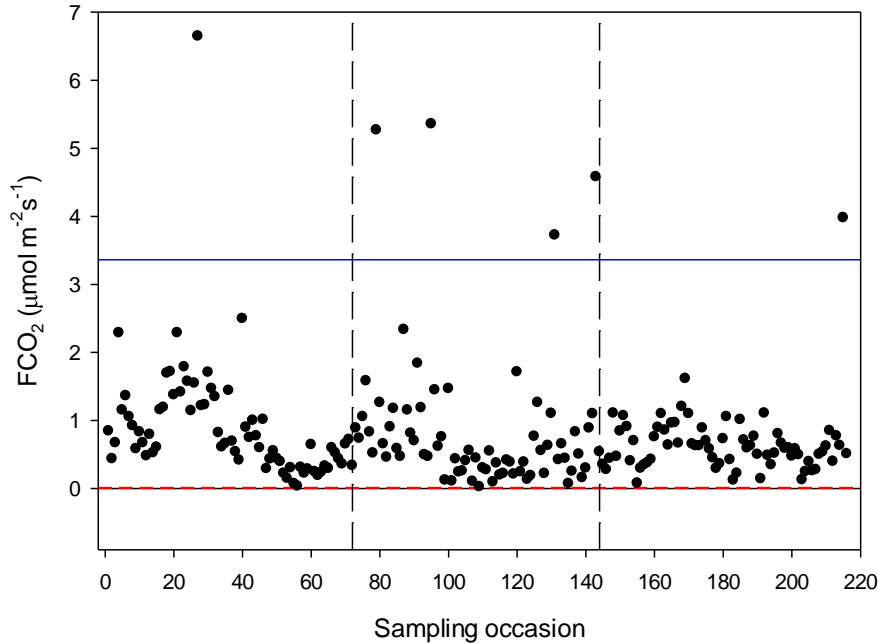
346
347   Figure 4. Measured CO_2 exchange (FCO_2) from the 24 sampling points using dark chamber and
348   portable gas analyzer. The dashed red line indicates CO_2 flux detection limit and the blue line
349   represents 3xS.D. of all data points. The dashed vertical lines separate sampling periods from left
350   to right: 14-15 June, 26 June – 2 July and 25-27 August, respectively.

351
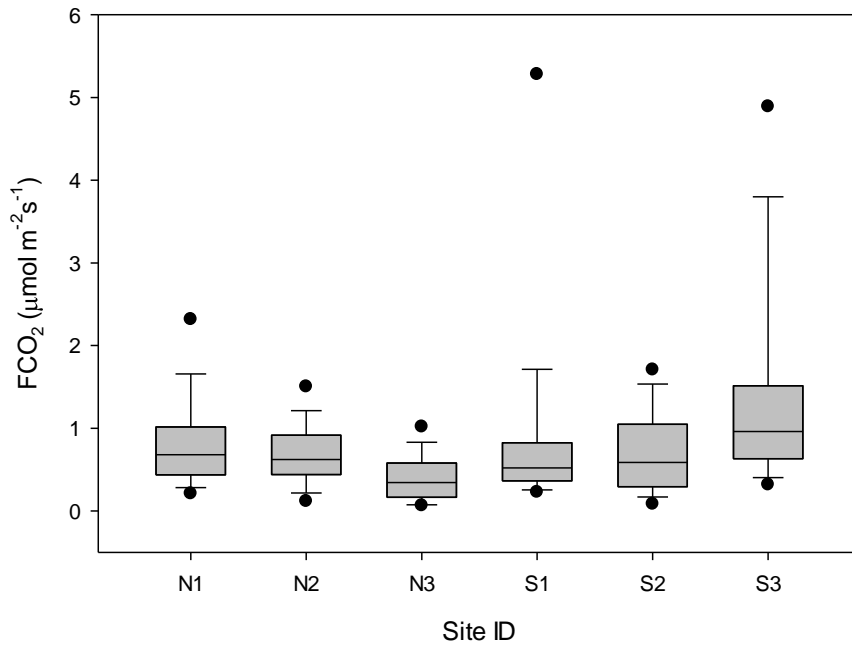
Figure 5. Box plot of CO_2 fluxes (FCO_2) per sampling location named N1-N3, S1-S3. The boundaries of the grey boxes represent the 25% and 75% percentiles, the line represent the median, whiskers above and below the boxes indicate the 10% and 90% percentiles. Outlaying points are also shown.

Of the tested environmental variables T_a, θ, T_s, ALD, S_{id} and GI it was only T_a, θ and GI that contributed positively and significantly in decreasing order to explain the variability of the CO_2 flux (Table 1).

Table 1. Result of stepwise linear regression with CO_2 flux as dependent variable. Normality test failed but significance in all variables was confirmed with Wilcoxon Signed rank tests. T_a is air temperature, θ is soil moisture and GI is green index.

Variable	Partial-R^2	Probability (p)
T_a	0.190	<0.001
θ	0.037	0.002
GI	0.023	0.002

Ideally all of these variables should be used in a model to estimate R_{eco} for gap filling purposes but we could only use air temperature since this was the only variable that we had access to with complete coverage for a full year. The Lloyd &Taylor model (Eq. 3 & Fig. 6)) was thus used to estimate ecosystem respiration for 2015 using half-hourly air temperature as input.
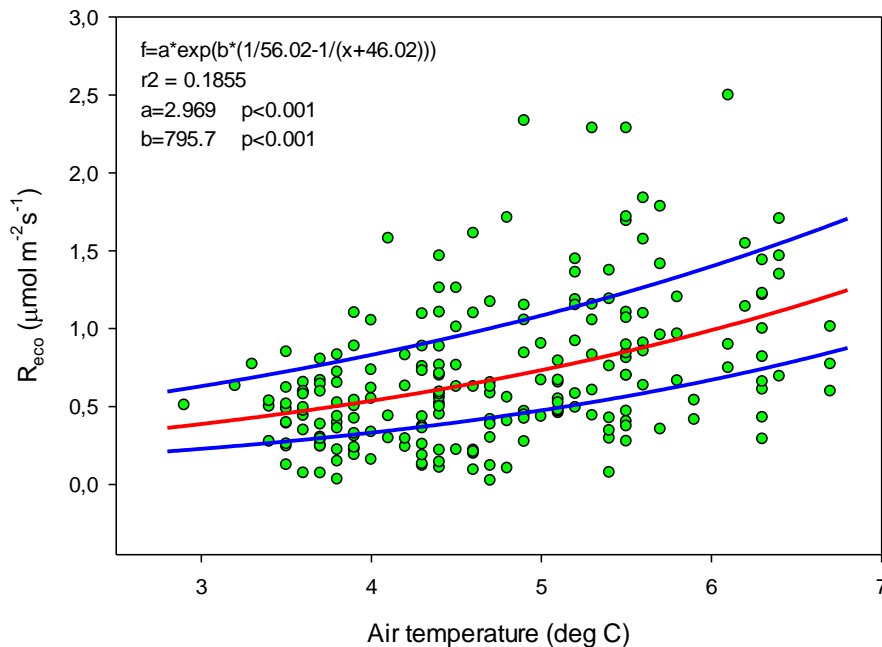
Figure 6. Measured ecosystem respiration (R_{eco}; green dots) using chambers plotted against air temperature. The red curve is the fitted equation and the blue curves are the corresponding boundaries when considering the standard deviation of the parameters.

375 The modelled gross primary productivity (Eq. 6; GPP_m) had a small offset when global radiation
376 was zero (Fig. 7). This offset was adjusted for when the model was applied for gapfilling so that
377 GPP become zero during nighttime.
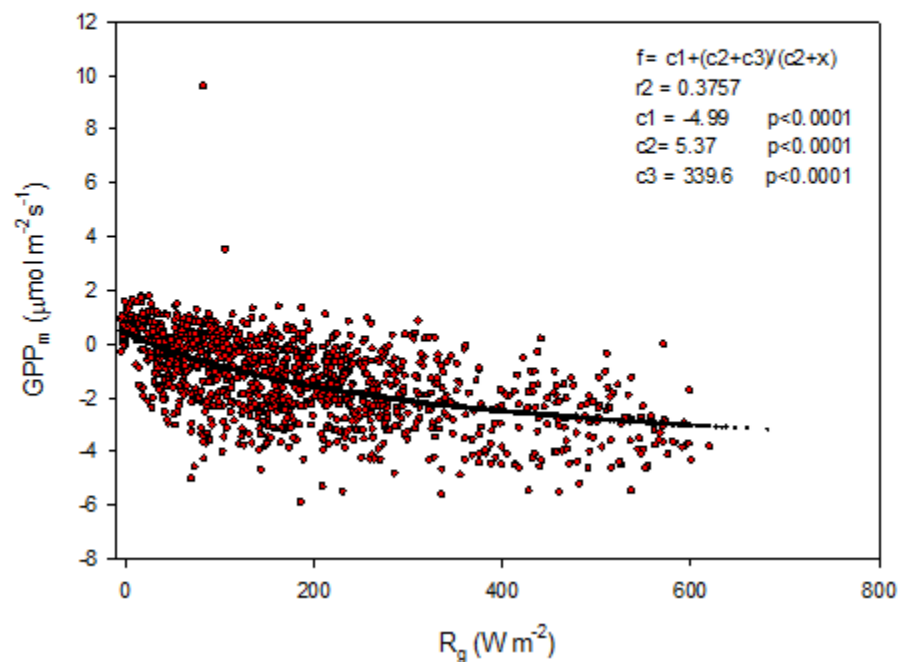
378
379
380 Figure 7. Gross primary productivity (GPP_m) plotted against global radiation (R_g); red symbols
381 are estimated values according to eq. (5) and the black symbols are the fitted model.

382
383
384
385
386
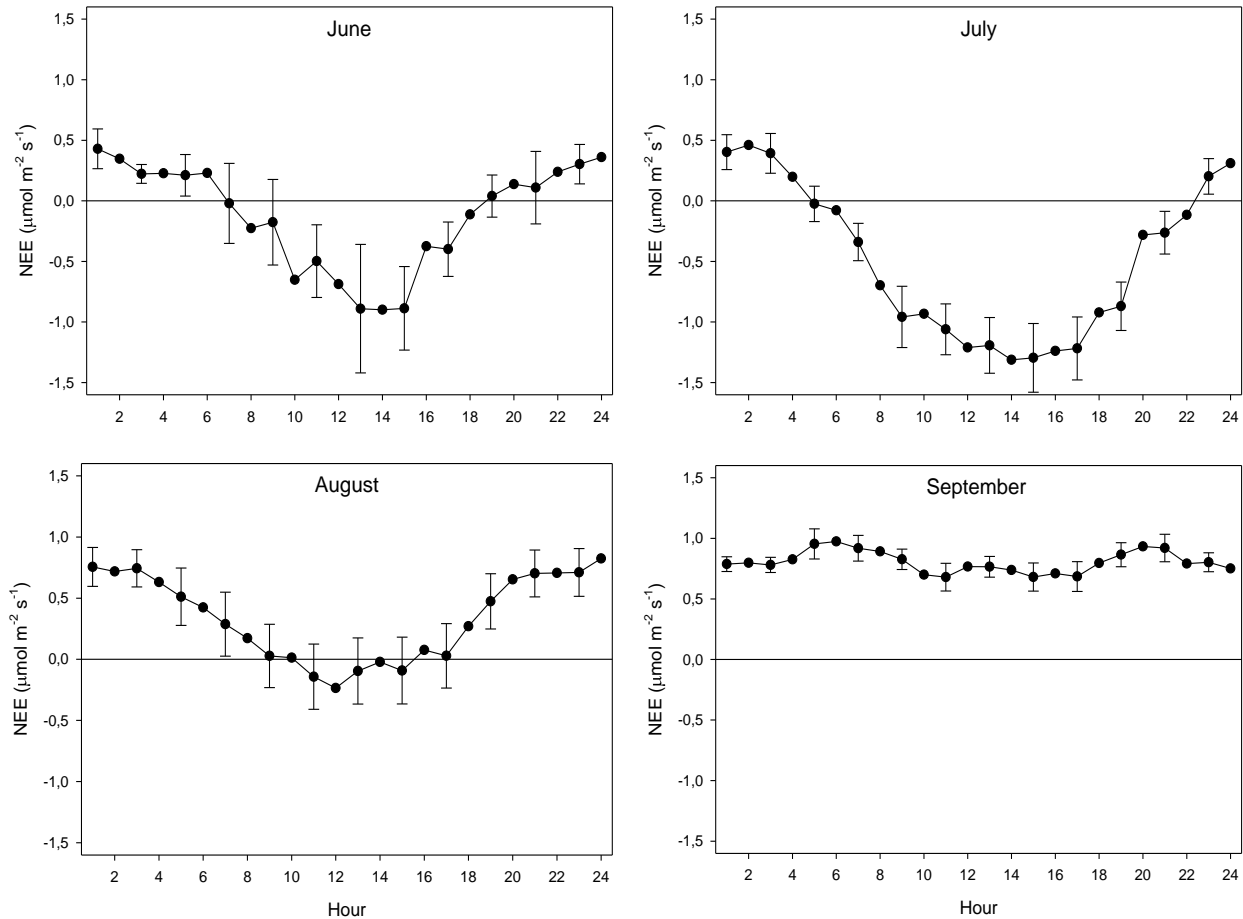
Figure 8. The mean monthly diurnal course of net ecosystem exchange (NEE) during the period of eddy covariance measurements 25 June to 17 September. The error bars (every 2nd shown) are the 95% confidence interval. Notice that the main part of August was gap filled because of measurement problems.

The diurnal course of NEE during June - August exhibit the normal pattern with a successively increasing drawdown of CO_2 during first half of the day resulting in a maximum around noon. It should be noted that during June until 20 August the sun was over the horizon 24 hours, thus no dark period. The positive values at the beginning and end of the diurnal courses are a result of R_{eco} being larger than GPP. As pointed out in Fig. 8, most of the data of August were gapfilled causing some additional uncertainty. However, the diurnal coure seems reasonable although the peak during noon is much lower as compared to July. This can be explained by the much lower incoming radiation in August as compared to July; the mean global radiation in July was 192 W m^{-2} and 98 W m^{-2} in August. The mean air temperature was similar during July and August. In September the incoming radiation is very low and thus GPP is also very low which result in a NEE that is dominated by the R_{eco}. The positive NEE values around mid-night during June – September are in good accordance with the values from the independent dark chamber measurements (Fig. 5).

408 In order to asses the impact of the large gap in measured data in August where we only had two
409 days of measured fluxes at the end of the month we made a comparison between the gap filled
410 diurnal course based on Wutzler et al. (2018) respectively our modelling using Eqs. 3 & 6. The
411 results show very good agreement between the two methods (see Supplemet) giving support to
412 the realism and reliability of the gap filled data.
413
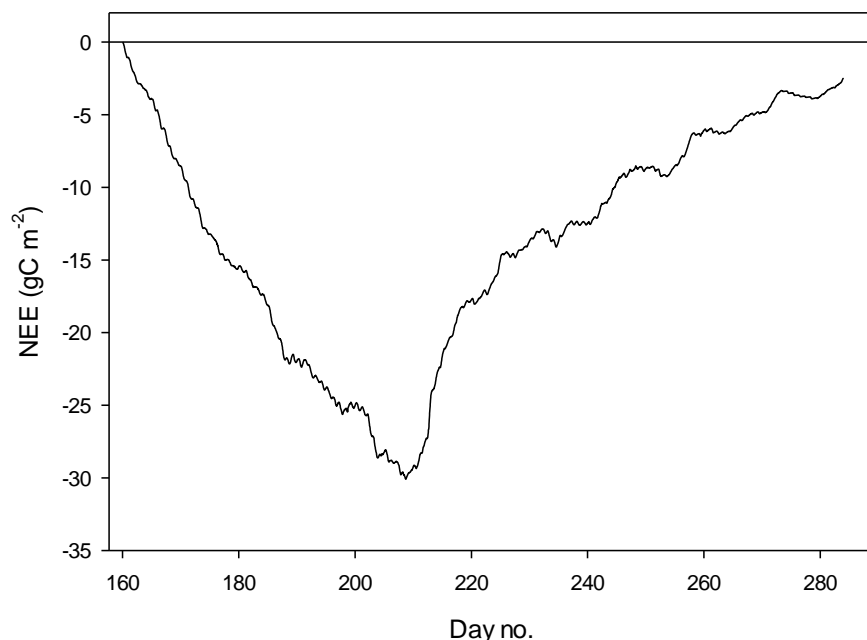
414
415 Figure 9. The cumulated half-hourly net ecosystem exchange (NEE) during growing season.
416
417 The mean net CO_2 flux during the growing season was -0.019 ± 0.024 µmol $m^{-2}s^{-1}$ with
418 uncertainty given as the 95% confidence limit. The cumulated NEE during growing season
419 ended up negative with -2.5 g C m^{-2} (Fig. 9). The mean net CO2 flux during summer was -
420 0.139 ± 0.032 µmol $m^{-2}s^{-1}$ (95% confidence limit) and the cumulated NEE was -11.8 g C m^{-2}
421 (Table 2).
422
423 Table 2. Summary of seasonal C-fluxes from Kapp Linne. R_{eco} is ecosystem respiration, GPP is
424 gross primary productivity and NEE is net ecosystem exchange.
425

Period	Component	Value (gC m^{-2})
Growing season	Reco	110.2
	GPP	-112.7
	NEE	-2.5
Summer	Reco	94.1
	GPP	-105.9
	NEE	-11.8

426
427 4.4 Temperature sensitivity of R_{eco} and GPP

428
429 The temperature sensitivity of the R_{eco} is already given by the fitted Lloyd & Taylor (1994)
430 equation. In the absence of long time series of measurements during multiple year were natural
431 climate variability could be used to assess temperature sensitivity of GPP we approached this
432 problem in the following way. We normalize GPP for its dependence on radiation by estimating
433 the difference between the 'measured' GPP and the model which only depends on radiation (see
434 Fig. 7). A stepwise linear regression with normalized GPP as dependent variable and air
435 temperature, time of season and vapour pressure deficit as independent variables, showed that of
436 the total explained variance, air temperature stood for 94% and time of season and and vapour
437 pressure deficit for 3% each.Thus, the resulting normalized GPP show effectively a dependence
438 on air temperature (Fig. 10) with values becoming more negative, i.e. showing increasing GPP
439 with increasing temperature. We fitted the same type of model to these data as for the R_{eco} to be
440 able to compare sensitivities to temperature.
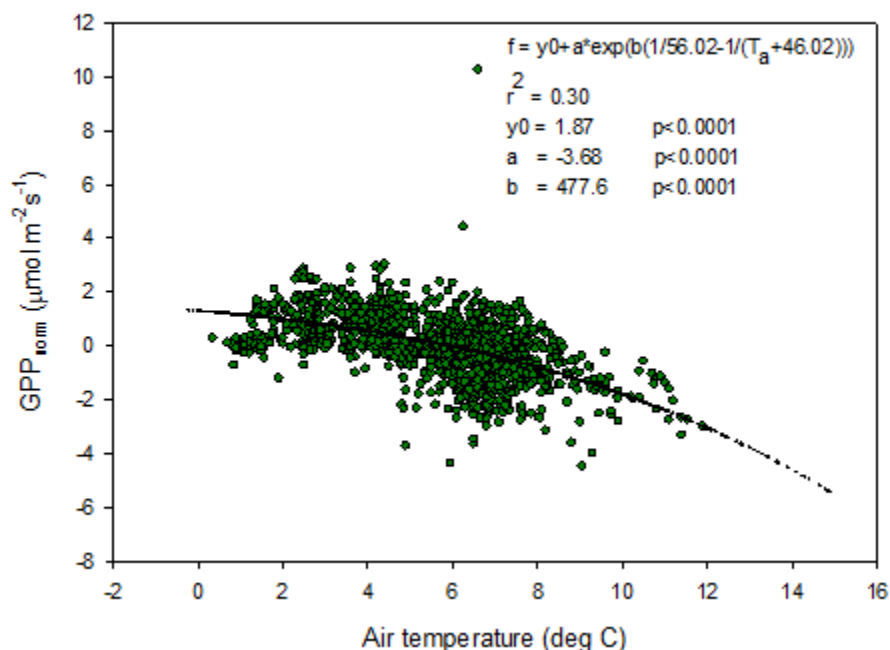
441
442 Figure 10. Normalized gross primary productivity (GPP) plotted against air temperature and with
443 the fitted exponential model.
444
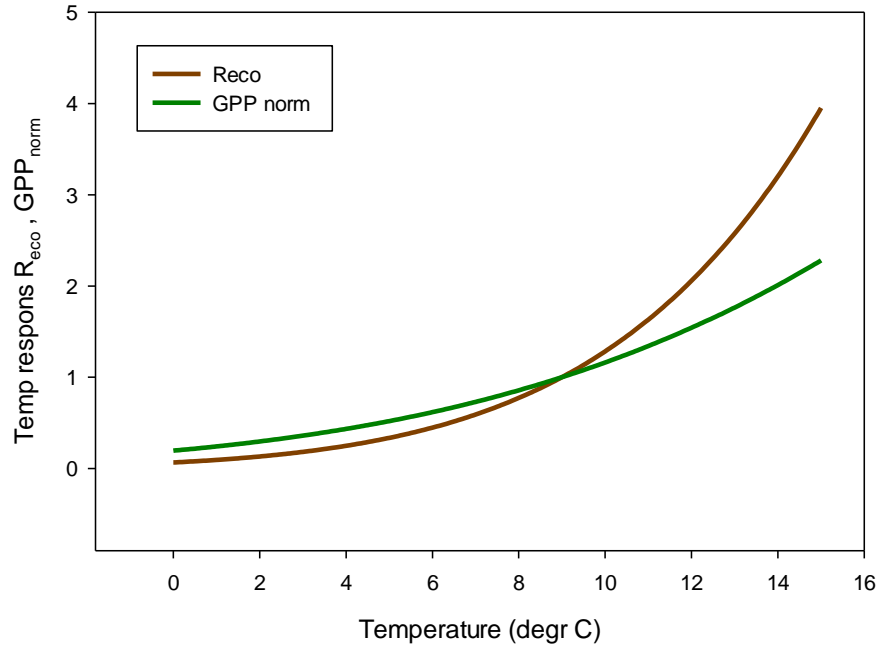
Figure 11. Temperature sensitivity for ecosystem respiration (R_{eco}) (brown) and R_g-normalized (positive) gross primary productivity (GPP) (green).

In Fig. 11 we reversed the sign of the GPP temperature response function to make it more easily comparable with the R_{eco} response model. The temperature sensitivity (μmol m^{-2}s^{-1} K^{-1}) can be estimated from the slope of these curves and the sensitivity is slightly higher for GPP than for R_{eco} in the interval 0 – 4.5 °C, thereafter the difference is small up to about 6 °C then it began to raise rapidly for R_{eco}. We tested what impact this could have by increasing the measured half-hourly air temperature by 1 °C and found that during the growing season the GPP increased by -31.9 g C m^{-2} and R_{eco} by 36.4 g C m^{-2}. Thus, a slightly larger increase of R_{eco} as compared to GPP resulting in that the small sink of -2.5 gC m^{-2} turns into a source of 4.5 gC m^{-2}.

4.5 CH$_4$ exchanges

The CH$_4$ fluxes from the chamber measurements showed large variation over time (Fig. 12) and across sampling locations (Fig. 13). The mean CH$_4$ flux of all samples was 0.00051±0.00024 μmol m^{-2}s^{-1}. The uncertainty is given as the 95% confidence limit. Setting all fluxes that fell within the flux detection limits to zero changed the mean value with -0.2%. Assuming that the mean flux was representative for the whole of growing season 1, the total CH$_4$ summer emission was 0.039 to 0.164 g CH$_4$ m^{-2}.

We also noticed a clear trend during the summer with highest fluxes in mid-June and then decreasing during the following two sampling occasions. The respective mean values with 95% confidence intervals for the three sampling periods were 0.00121±0.000512 μmol m^{-2}s^{-1}(June 14-15), 0.000332±0.000465 μmol m^{-2}s^{-1}(June 26- July 2) and -0.00000781±0.0000936 μmol m^{-2}s^{-1}(August 25-26).

473 For CH$_4$ exchanges we found *ALD,* θ and *GI* to contribute significantly to explain the variance of
474 the flux (Table 3). The CH$_4$ flux responded negatively to increasing ALD and positively to θ and
475 *GI*.
476
477 Table 3. Result of stepwise multiple linear regression with CH$_4$ flux as dependent variable.
478 Normality test failed but significance in all variables was confirmed with Wilcoxon Signed rank
479 tests. ALD is active layer depth, θ is soil moisture and GI is green index.
480

Variable	Delta-R^2	Probability (p)
ALD	0.175	<0.001
θ	0.025	0.01
GI	0.020	0.004

481
482
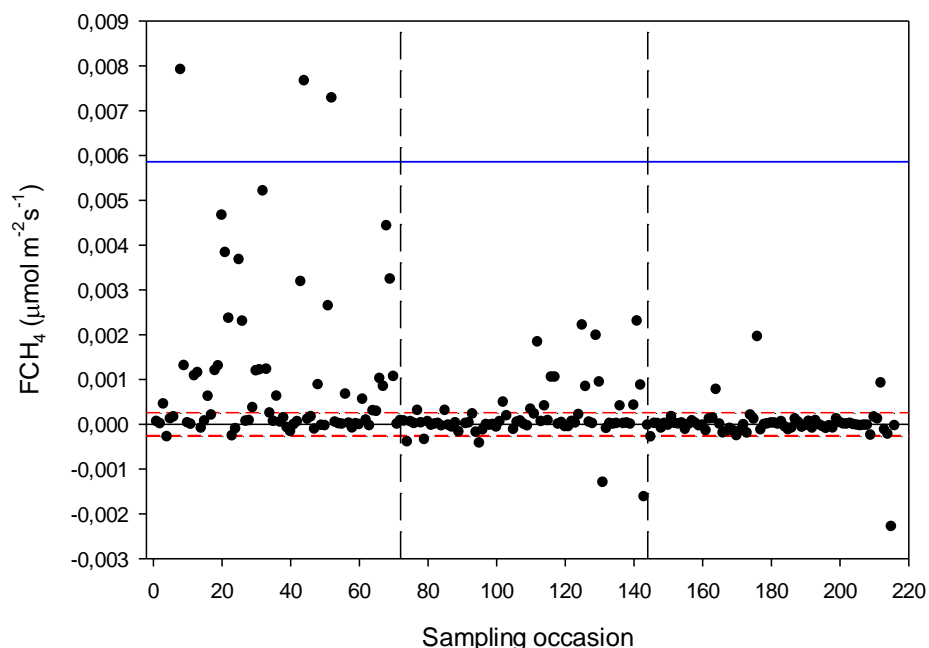
483
484 Figure 12. Measured CH$_4$ exchange (FCH$_4$) from the 24 sampling points using dark chamber and
485 portable gas analyzer. The dashed red lines indicate CH$_4$ flux detection limit, (i.e. inside the
486 limits of detection the exact numbers are highly uncertain) and the blue line represents 3xS.D.
487 The dashed vertical lines – same as in Fig. 4.

488
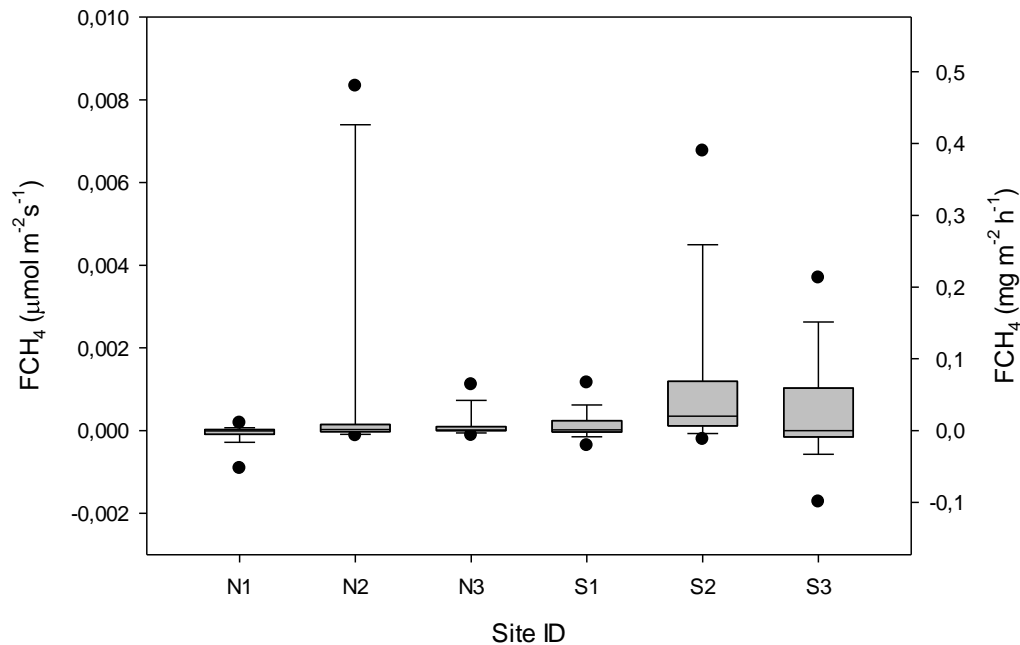
Figure 13. Box plot of CH_4 fluxes (FCH_4) per sampling location named N1-N3, S1-S3. The
statistics includes also the data that fall within the flux detection limits. The boundaries of the
grey boxes represent the 25% and 75% percentiles, the line represent the median, whiskers above
and below the boxes indicate the 10% and 90% percentiles. Outlaying points are also shown.

5 Discussion

5.1 Seasonal CO_2 fluxes

We focus our discussion mainly on comparison with other tundra sites located in the North
Atlantic area since these sites are influenced by the North Atlantic Current with its impact on
weather patterns and climate. This limits the comparisons to sites in Greenland, Svalbard and
Northern Scandinavia. However, we broaden the comparison a bit by adding two sites from
Alaska.

Lund et al. (2012) found that the start of the uptake period was strongly correlated with start of
the snowmelt for the fen in Zackenberg, NE Greenland. They defined the start of snowmelt as
the day when snow depth was <0.1 m. This coincides very well with our definition of start of
growing season (see Fig. 2). Our results for the growing season NEE showing a small net uptake
of -2.5 g C m^{-2} is at the low end in comparison with any other high artic sites which all show a
larger gain of carbon during the growing seasons.

Lund et al. (2012) analysed 10 years of EC flux measurements from a heathland in Zackenberg
and they reported a NEE range of -39.7 to -4.3 g C m^{-2} for the growing season. It was only two
years out of ten that showed NEE values close to zero but still indicating a small net uptake in
Zackenberg heath. Their measured growing season GPP was in the range of -95.4 to -54.1 g C m^{-2}
and the R_{eco} was in the range of 37.7 to 63.8 g C m^{-2}. Our corresponding values were -112.7 g

514 C m^{-2} for GPP and 110.2 g C m^{-2} for R$_{eco}$. López-Blanco et al. (2017) presented data over a
515 period of eight years of EC flux measurements from Kobbefjord, SW Greenland over an area of
516 mixed fen and heath vegetation. Their growing season ranges were; for NEE -74.2 to -45.9 g C
517 m^{-2}, for GPP -316.2 to – 181.8 g C m^{-2} and for R$_{eco}$ it was 144.2 to 279.2 g C m^{-2} excluding 2011
518 which was anomalous because of a pest outbreak and 2014 which did not have a full growing
519 season.

521 Our estimate of a small summer NEE of -11.8 g C m^{-2} (Table 2) is also different in comparison
522 with other tundra sites which show larger uptake during the summer; for a fen type of vegetation
523 in NE Greenland Soegaard and Nordstroem (1999) reported -96.3 g C m^{-2} while Rennermalm et
524 al. (2005) reported -50 g C m^{-2} for the same site but for a different year. Groendahl et al. (2007)
525 reported a range of -1.4 to -18.9 g C m^{-2} for heath vegetation also on NE Greenland.

527 It is difficult to compare growing season values firstly because they are rarely defined the same
528 way. Only small differences in definition of start and end of growing season can have a large
529 impact on the NEE values since NEE is the sum of two large components of almost equal size
530 and of different sign. Secondly, it is also difficult to compare GPP and R$_{eco}$ for any season since
531 the methods to split NEE into components differ from case to case. The most reliable comparison
532 is probably for summer season (June – August) since most studies represents this period best in
533 terms of measurement coverage and quality. And thirdly, there are differences in vegetation type
534 that can have a big impact on gas exchanges. Our moist moss tundra is dominated by moss
535 species and mosses are not as efficient primary producers as vascular plants and this make the
536 net uptake of carbon dioxide small as compared to heath or wet fen systems.

538 The climate warming is predicted to be most evident at high latitudes such as the Arctic region.
539 Svalbard has experienced significant warming during the last decades (1971-2017) with 3- 5
540 degrees with the largest increase in the winter and smallest in the summer (Hanssen-Bauer et al.,
541 2019). Our air temperature observations in 2015 are in line with these results (Fig.1). An
542 interesting question is if such changes in temperature has also affected the net carbon balance of
543 the ecosystem? Our analysis of temperature sensitivity of R$_{eco}$ and GPP shows that this could be
544 the case for this site since R$_{eco}$ is increasing more than GPP for temperatures above about 6 ℃
545 which occurs quite frequent during the summer (see Fig. 2). Our analyses of the impact of a
546 temperature increase of 1 ℃ showed that our small sink of -2.5 g C m^{-2} during growing season
547 would be turned into a similarly small source of 4.5 g C m^{-2} for a 1 degree increase in air
548 temperature. These results are in line of those of Welker et al. (2004) who performed a warming
549 experiment in high Arctic tundra ecosystems. They showed that the net ecosystem exchange in
550 the wet tundra ecosystem decreased by 20% during growing season under a 2 degree warming
551 treatment. This was in contrast to the dry and mesic ecosystems which increased their net carbon
552 uptake by 12-30%.

555   5.2 CH$_4$ fluxes

557 Our estimated growing season CH$_4$ flux of 0.08 g C m^{-2} is very low compared to most other
558 methane emitting tundra sites; the Zackenberg fen site emitted CH$_4$ in the range 1.4 to 4.9 g C m^{-}
559 ^{2} (Mastepanov et al. (2013), Jackowicz-Korczynski et al. (2010) and Jammet et al. (2015)

560 reported 20.1 to 25.1 g CH_4 m^{-2} for the Stordalen mire in Northern Sweden. For three different
561 sites in northern Alaska, Bao et al. (2021) reported annual emissions between 1.8 and 8.5 g CH_4
562 m^{-2} which corresponds to 0.94 and 4.5 g CH_4 m^{-2} for the growing season based on their estimate
563 that growing season emissions are 52.6% of the annual emissions. Sachs et al. (2008) measured
564 CH_4 exchanges with EC method in a northern Siberian polygon tundra and found generally low
565 fluxes of about 18.5 mg CH_4 m^{-2} day^{-1} with little variation over the growing season. This rate
566 adds up to 2.3 g CH_4 m^{-2} for their four months long growing season.
567
568 It should be pointed out that we did not perform measurements during the shoulder seasons
569 meaning that we probably underestimate the seasonal total. Importance of shoulder seasons was
570 first pointed out by Mastepanov et al. (2008) which discovered a large burst of CH_4 at and after
571 the onset of soil freezing. One interesting observation is that the main part of our CH_4 flux
572 occurred during the sampling period 14-15 June 2016 which is about 30 days after snow melt.
573 This is the time of the season when CH_4 emissions normally are peaking (Mastepanov et al.
574 2013). After that, the rates dropped to practically zero in late August (see Fig. 12).
575
576
577 The comparison between the different sites are hampered by the fact that they in most cases
578 belong to different bioclimatic subzones with differences in climate and vegetation (Walker et
579 al., 2005). The only site besides Kapp Linne that belong to subzone B is the one in Ny Ålesund.
580 The other high Arctic sites Adventdalen and Zackenberg both belong to subzone C, the
581 intermediate high/low Arctic sites Kobbefjord and Disco Island belongs to subzone D
582 respectively C/D. The low Arctic site Atqasuk belong to subzone D and the Imnavait Creek
583 belong to subzone E. The sub-Arctic Abisko is not classified by Walker et al. (2005) but based
584 mean July air temperature it should belong to subzone E. These differences in climate and
585 vegetation should be kept in mind when comparing results from different sites.
586
587   5.3 Environmental controls of fluxes
588
589 A key issue in high Arctic is how ecosystems with soil that contain large amounts of frozen
590 carbon will respond to warming. A recent report about the future climate of Svalbard (Hanssen-
591 Bauer et al. 2019) show that appalling changes are at risk to occur. By 2071-2100 compared to
592 1971-2000 the mean annual temperature is estimated to increase by 7 ℃ to 10 ℃ for the medium
593 and high emission scenarios, respectively. Precipitation is also estimated to increase by 45%
594 respectively 65% for these scenarios. Such large changes will of course also have a lot of other
595 impacts as well for instance shorter snow season, more erosion and sediment transport, changes
596 in vegetation composition and growth etc etc. Assessment of such large changes are very
597 difficult and is far beyond the scope of this paper. We have however shown that for a smaller
598 temperature increase of 1 degree, the impact on the net carbon balance during the growing
599 season will be minute; the increase in ecosystem respiration is compensated for by a
600 corresponding, or actually slightly larger increase of gross primary productivity. Similar
601 compensation effect was obtained for a heath site in Zackenberg by Lund et al. (2012). They
602 used multi-year measurements to assess the effect of changes in temperature on the growing
603 season fluxes
604

605 We found that air temperature was the main control of ecosystem respiration followed by soil
606 moisture and greenness index (Table 1). We had expected that soil temperature should contribute
607 significantly to explain the variations in R_{eco} but it did not. Cannone et al. (2019) showed that
608 ground surface temperature at 2 cm depth contributed significantly to explain R_{eco} in nearby
609 Adventdalen during early, peak and late parts of the growing season. In their study soil moisture
610 was also significant during peak and late seasons. One possible explanation to this difference in
611 responses could be that our soil temperature was measured at 5 cm depth and that air temperature
612 was more representative for the microbial processes taking place in or near the soil surface.
613 Interestingly, GI contributed significantly to explain variations in R_{eco}. The GI was clearly
614 correlated with the abundance of *Salix polaris* (see Supplement) and thus we interpret the
615 positive correlation between GI and R_{eco} to be an effect of increasing contribution by autotrophic
616 respiration to the total respiration.

617 We found no significant correlation between CH_4 emission and temperature. The best
618 explanation was by active layer depth followed by soil moisture and GI (Table 3). But it should
619 be pointed out that ALD and θ are not independent from each other and that ALD can be
620 regarded as a proxy for any seasonal variability, like plant phenology. Soil moisture decreases
621 with increasing active layer depth. The correlation between GI and CH_4 emission is probably
622 also connected with abundance of the vascular plant *Salix polaris*. Vascular plants are since long
623 mentioned as a pathway for CH_4 from the soil interior to the atmosphere in wet tundra
624 ecosystems (e.g. Schimel, 1995) but it could also be an effect of mediation of soil by the root
625 exudation of organic acids as mentioned by Ström et al. (2012). However, we have not found any
626 studies supporting the latter hypothesis concerning Salix polaris.

627 **6 Conclusions**

628 Our analyses of EC and chamber flux measurements have shown that the moss tunda on Kapp
629 Linne is a small sink of CO_2 and a small source of CH_4 during the growing season. Realizing that
630 the winter season also emit CO_2, we tentatively conclude that this moist moss tundra is a source
631 on an annual basis. Concerning the magnitude of the CO_2 exchanges during summer we find it to
632 be anomalous compared to fens and heath ecosystems located in the North Atlantic region
633 which all are sinks during the summer. The CH_4 exchange is much lower than for other tundra
634 ecosystems in the region.
635
636 The temperature sensitivity for CO_2 exchange was slightly higher for GPP than for R_{eco} in the
637 low temperature range of 0-4.5 ºC, almost similar up to 6 ºC and thereafter it was considerably
638 higher for R_{eco}. The consequence of this, for a small increase in air temperature of 1 degree (all
639 other variables assumed unchanged) was that the respiration increased more than photosynthesis
640 turning the small sink into a small source. But a warmer winter period would probably also result
641 in an additionally increased loss of carbon. We cannot rule out that the reason why the moss
642 tundra is close to balance today is an effect of the warming that has already taken place in
643 Svalbard.

644 The analysis of which environmental factors that controlled the small-scale fluxes showed that
645 air temperature dominated for R_{eco} and active layer depth for CH_4 but we also found that
646 greenness index significantly explained part of the variation in these fluxes. For R_{eco} we
647 attributed this to an increased share of autotrophic respiration to the total and for CH_4 we

hypothesized that the abundance of the dwarf shrub *Salix polaris* effected the exchange either through internal plant pathway for methane or through increased provision of C substrate to the anaerobic microbial community stimulating the production of methane. This finding is an indication that modeling of CO_2 as well as of CH_4 fluxes can be improved by also considering differences and changes in greenness of the vegetation.

7 Supplement

The supplement contains some additional photographs of equipment, site and color photograps of vegetation within the frames used for chamber measurements.

8 Data availability

Data can be obtained from https://zenodo.org (10.5281/zenodo.5704508).

9 Author contribution

AL designed the study and wrote the manuscript. NP and AL performed the EC measurements and analysed the EC data. ISJ did the vegetation characterization. AL, CS, LK and MBN performed the chamber measurements. All authors have read and commented the manuscript.

10 Competing interests

We declare no competing interests.

11 Acknowledgments

This work did not receive any other funding except salaries for the authors from their respective organizations. Observations of air temperature, relative humidity, precipitation, ground ice conditions and snow depth were obtained from Norwegian Centre for Climate Services (NCCS) and provided under licence CC BY 4.0. Global radiation data from Adventdalen was obtained from the University Centre in Svalbard (UNIS). Thanks to associated professor Jonas Åkerman, Lund University for support with information about the site.

12 References

Arias, P. A., Bellouin, E., Coppola, R.G. et al.: Technical Summary, in: Climate Change 2021: The Physical Science Basis. Contribution of Working Group I to the Sixth Assessment Report of the Intergovernmental Panel on Climate Change, edited by: Masson-Delmotte, V., P. Zhai, A. Pirani, S. L. Connors, C. Péan, S. Berger, N. Caud, Y. Chen, L. Goldfarb, M. I. Gomis, M. Huang, K. Leitzell, E. Lonnoy, J.B.R. Matthews, T. K. Maycock, T. Waterfield, O. Yelekçi, R. Yu and B. Zhou, Cambridge University Press, In Press, 2021.

Bao, T., Xu, X., Jia, G., Billesbach, D.P. and Sullivan, R.C.: Much stronger tundra methane emissions during autumn freeze than spring thaw, Global Change Biology, 27, 376–387, https://doi.org/ 10.1111/gcb.15421, 2021

Bosiö, J., Stiegler, C., Johansson, M., Mbufong, H. N. and Christensen, T. R.: Increased photosynthesis compensates for shorter growing season in subarctic tundra—8 years of

684   snow accumulation manipulations, Climatic Change, 127, 321–334,
685   http://doi.org/10.1007/s10584-014-1247-4, 2014.

686 Burba, G. G., McDermitt, D., Grelle, A., Anderson, D.J. and Xu, L.: Addressing the influence of
687   instrument surface heat exchange on the measurements of CO_2 flux from open-path gas
688   analyzers, Global Change Biology, 14, 1854–1876, https://doi.org/10.1111/j.1365-
689   2486.2008.01606.x, 2008.

690 Callaghan, T.V., Björn, L O., Chapin III, F.S., Chernov, Y., Christensen, T.R., Huntley, B., Ims,
691   R., Johansson, M., Jolly Riedlinger, D., Jonasson, S., Matveyeva, N., Oechel, W.,
692   Panikov, N. and Shaver, G.: Arctic tundra and polar desert ecosystems, in: Arctic Climate
693   Impact Assessment, edited by: ACIA, Cambridge University Press, 243-352, 2005.

694 Cannonea, N., Pontib, S., Christiansen, H.H., Christensen, T.R., Pirk, N. and Guglielmin, M.:
695   Effects of active layer seasonal dynamics and plant phenology on CO_2 land atmosphere
696   fluxes at polygonal tundra in the High Arctic, Svalbard, Catena, 174, 142-153,
697   https://doi.org/ 10.1016/j.catena.2018.11.013, 2019.

698 Christensen, T.R., Johansson, T., Akerman, H.J. and Mastepanov, M.: Thawing sub-arctic
699   permafrost: Effects on vegetation and methane emissions, Geophysical Research Letters,
700   31, L04501, https://doi.org/10.1029/2003GL018680, 2004.

701 Christensen, T.R., Jackowicz-Korzynski, M., Aurela, M., Crill, P., Heliasz, M., Mastepanov, M.
702   and Friborg, T.: Monitoring the Multi-Year Carbon Balance of a Subarctic Palsa Mire
703   with Micrometeorological Techniques, Ambio, 41, 207–217,
704   https://doi.org/10.1007/s13280-012-0302-5, 2012.

705 Dobler, A., Lutz, J., Landgren, O. and Haugen, J. E.: Circulation Specific Precipitation Patterns
706   over Svalbard and Projected Future Changes, Atmosphere, 11, 1378;
707   doi:10.3390/atmos11121378, 2021.

708

709 Euskirchen, E. S., Bret-Harte, M. S., Scott, G. J., Edgar, C., and Shaver, G. R.: Seasonal patterns
710   of carbon dioxide and water fluxes in three representative tundra ecosystems in northern
711   Alaska, Ecosphere, 3, 1–19, https://doi.org/10.1890/ES11-00202.1, 2012.

712

713 Euskirchen, E.S., Bret-Harte, M.S., Shaver, G.R., Edgar, C.W., and Romanovsky, V.E.: Long-
714   Term Release of Carbon Dioxide from Arctic Tundra Ecosystems in Alaska, Ecosystems,
715   20, 960–974, http://doi.org/10.1007/s10021-016-0085-9, 2017.

716 Friedlingstein, P., Cox, P., Betts, R., Bopp, L., von Bloh, W., Brovkin, V., Cadule, P., Doney, S.,
717   Eby, M., Fung, I., Bala, G., John, J., Jones, C., Joos, F., Kato, T., Kawamiya, M., Knorr,
718   W., Lindsay, K., Matthews, H. D., Raddatz, T., Rayner, P., Reick, C., Roeckner, E.,
719   Schnitzler, K. G., Schnur, R., Strassmann, K., Weaver, A. J., Yoshikawa, C., and Zeng,

N.: Climate-carbon cycle feedback analysis: Results from the C4MIP model
intercomparison, J. Climate, 19, 3337–3353, https://doi.org/10.1175/JCLI3800.1, 2006.

Friedlingstein, P., O'Sullivan, M., Jones, M.W. et al.: Global carbon budget 2010, Earth Syst.
Sci. Data, 12, 3269–3340, https://doi.org/10.5194/essd-12-3269-2020, 2019.

Groendahl, L., Friborg, T., and Soegaard, H.: Temperature and snow-melt controls on
interannual variability in carbon exchange in the high Arctic, Theor. Appl. Climatol., 88,
111–125, http://doi.org/10.1007/s00704-005-0228-y, 2007.

Hanssen-Bauer, I., Førland, E.J., Hisdal, H., Mayer, S., Sandø, A.B. and Sorteberg, A.:Climate in
Svalbard 2100 – a knowledge base for climate adaptation, Norwegian Environment
Agency, Report no. 1/2019., 2019.

Hugelius, G., Strauss, J., Zubrzycki, S., Haren, J.W., Schuur, E.A.G., Ping, C.-L., Schirrmeister,
L., Grosse, G., Michaelson, G.J., Koven, C.D., O'Donnell, J.A., Elberling, B., Mishra,
U., Camill, P., Yu, Z., Palmtag, J. and Kuhry, P.: Estimated stocks of circumpolar
permafrost carbon with quantified uncertainty ranges and identified data gaps,
Biogeosciences, 11, 6573–6593, http://doi.org/10.5194/bg-11-6573-2014, 2014.

Jackowicz-Korczynski, M., Christensen, T. R., Backstrand, K., Crill, P., Friborg, T.,
Mastepanov, M. and Strom, L.: Annual cycle of methane emission from a subarctic
peatland, J. Geophys. Res.-Biogeo., 115, G02009, http://doi.org/10.1029/2008JG000913,
2010.

Jammet, M., Crill, P., Dengel, S. and Friborg, T.: Large methane emissions from a subarctic
lake during spring thaw: Mechanisms and landscape significance. J. Geophys. Res.-
Biogeo., 120, 2289-2305, http://doi.org/10.1002/2015JG003137, 2015.

Kljun, N., Calanca, P., Rotach, M.W., and Schmid, H.P.: A simple two-dimensional
parameterisation for Flux Footprint Prediction (FFP), Geosci. Model Dev., 8, 3695-3713,
http://doi.or/10.5194/gmd-8-3695-2015, 2015.

Lasslop, G., Reichstein, M., Papale, D., Richardson, A., Arneth, A., Barr, A., Stoy, P. and
Wohlfahrt, G.: Separation of net ecosystem exchange into assimilation and respiration
using a light response curve approach: critical issues and global evaluation. Global
Change Biology, 16, 187-208, https://doi.org/10.1111/j.1365-2486.2009.02041.x, 2010.

Li-Cor: EddyPro® Software (Version 6.0), Li-Cor Inc., Lincoln, USA, 2016.

Lloyd, J., and Taylor, J.A.: On the temperature dependence of soil respiration, Functional
Ecology, 8(3), 315-323, 1994.

Lopez-Blanco, E., Lund, M., Williams, M., Tamstorf, M.P., Westergaard-Nielsen, A., Exbrayat,
J.-F., Hansen, B.U., and Christensen, T.R.: Exchange of CO_2 in Arctic tundra: impacts of

meteorological variations and biological disturbance, Biogeosciences, 14, 4467–4483, https://doi.org/10.5194/bg-14-4467-2017, 2017.

Lund, M., Falk, J. M., Friborg, T., Mbufong, H. N., Sigsgaard, C., Soegaard, H., and Tamstorf, M. P.: Trends in CO2 exchange in a high Arctic tundra heath, 2000–2010, J. Geophys. Res.- Biogeo., https://doi.org/10.1029/2011JG001901, 2012.

Lüers, J., Westermann, S., Piel, K., and Boike, J.: Annual CO2 budget and seasonal CO2 exchange signals at a high Arctic permafrost site on Spitsbergen, Svalbard archipelago, Biogeosciences, 11, 6307–6322, http://doi.0rg/10.5194/bg-11-6307, 2014.

Mastepanov, M., Sigsgaard, C., Dlugokencky, E. J., Houweling, S., Strom L., Tamstorf, M. P., and Christensen, T. R.: Large tundra methane burst during onset of freezing, Nature, 456, 628–631, http://doi.org/10.1038/nature07464, 2008.

Mastepanov, M., Sigsgaard, C., Tagesson, T., Ström, L., Tamstorf, M. P., Lund, M., and Christensen, T. R.: Revisiting factors controlling methane emissions from high-Arctic tundra, Biogeosciences, 10, 5139–5158, https://doi.org/10.5194/bg-10- 5139-2013, 2013.

McGuire, A. D., Christensen, T. R., Hayes, D., Heroult, A., Euskirchen, E., Kimball, J. S., Koven, C., Lafleur, P., Miller, P. A., Oechel, W., Peylin, P., Williams, M., and Yi, Y.: An assessment of the carbon balance of Arctic tundra: comparisons among observations, process models, and atmospheric inversions, Biogeosciences, 9, 3185–3204, https://doi.org/10.5194/bg-9-3185- 2012, 2012.

Myers-Smith, I. H., Kerby, J. T., Phoenix, G. K., Bjerke, J. W., Epstein, H. E., Assman, J. J., John, C., Adreu-Hayles, L., Angers-Blondin, S., Beck, P. S. A., Berner, L. T., Bhatt, U. S., Bjorkman, A. D., Blok, D., Bryn, A., Christiansen, C. T., Cornelissen, J. H. C., Cunliffe, A. M., Elmendorf, S. C., Forbes, B. C., Goetz, S. J., Hollister, R. D., de Jong, R., Loranty, M. M., Marcias-Fauria, K., Maseyk, K., Normand, S., Olofsson, J., Parker, T. C., Parmentier, F-J. W., Post, E., Schaepman-Strub, G., Stordal, F., Sullivan, P. F., Thomas, H. J. D., Tømmervik, H., Treharne, R., Tweedie, C. E., Walker, D. A., Wilmking, M. and Wipf, S.: Complexity revealed in the greening of the Arctic, Nat. Clim. Chang., 10, 106–117, https://doi.org/10.1038/s41558-019-0688, 2020.

Oechel, W. C., C. A. Laskowski, G. Burba, B. Gioli, and Kalhori, A.A.M.: Annual patterns and budget of CO2 flux in an Arctic tussock tundra ecosystem, J. Geophys. Res. Biogeosci., 119, 323–339, http://doi.org/10.1002/2013JG002431, 2014.

Pastorello, G., Trotta, C., Canfora, E. et al.: The FLUXNET2015 dataset and the ONEFlux processing pipeline for eddy covariance data, Sci Data, 7, 225, https://doi.org/10.1038/s41597-020-0534-3, 2020.

Pirk, N., Sievers, J., Mertes, J., Parmentier, F.-J. W., Mastepanov, M., and Christensen, T. R.: Spatial variability of CO_2 uptake in polygonal tundra: assessing low-frequency

790   disturbances in eddy covariance flux estimates, Biogeosciences, 14, 3157–3169,
791   https://doi.org/10.5194/bg-14-3157-2017, 2017.

792 Post, E., Forchhammar, M. C., Bret-Harte, M. S., Callaghan, T. V., Christensen, T. R., Elberling,
793   B., Fox, A. D., Gilg, O., Hik, D. S., Høye, T. T., Ims, R. A., Jeppesen, E., Klein, D. R.,
794   Madesn, J., McGuire, A. D., Rysgaard, S., Schindler, D. E., Stirling, I., Tamstorf, M. P.,
795   Tyler, N. J. C., van der Wal, R., Welker, J., Wookey, P. A., Schmidt, M. and Astrup, P.:
796   Ecological dynamics across the arctic associated with recent climate change, Science,
797   325, 1355–1358, http://doi.org/10.1126/science.117311, 2009.

798 Ravolainen, V., Soininen, E. M., Jónsdóttir, I. S., Eischeid, I., Forchhammer, M., van der Wal,
799   R. and Pedersen, A. Ø.: High Arctic ecosystem states: Conceptual models of vegetation
800   change to guide long-term monitoring and research, Ambio, 49, 666–677,
801   https://doi.org/10.1007/s13280-019-01310-x, 2020.

802 Rennermalm, A.K., Soegaard, H., and Nordstroem, C.: Interannual Variability in Carbon
803   Dioxide Exchange from a High Arctic Fen Estimated by Measurements and Modeling,
804   Arctic, Antarctic, and Alpine Research, 37(4), 545-556, https://doi.org/10.1657/1523-
805   0430(2005)037[0545:IVICDE]2.0.CO;2, 2005.

806 Richardson, A. D., Braswell, B. H., Hollinger, D. Y., Jenkins, J. P. and Ollinger, S. V.: Near-
807   surface remote sensing of spatial and temporal variation in canopy phenology, Ecological
808   Applications, 19, 1417–1428, http://doi.org/10.1890/08-2022.1, 2009.

809 Sachs, T., Wille, C., Boike, J., and Kutzbach, L.: Environmental controls on ecosystem-scale
810   CH_4 emission from polygonal tundra in the Lena river delta, Siberia, J. Geophys. Res.-
811   Biogeosci., 113, G00A03, http://doi.org/10.1029/2007JG000505, 2008.

812 Saunois, M., Stavert, A.R., Poulter, B et al.: The global methane budget 2000-2017, Earth Syst.
813   Sci. Data, 12, 1561–1623, https://doi.org/10.5194/essd-12-1561, 2020.

814 Schimel, J.P.: Plant Transport and Methane Production as Controls on Methane Flux from Arctic
815   Wet Meadow Tundra, Biogeochemistry, 28 (3), 183-200,
816   https://doi.org/10.1007/BF02186458, 1995.

817 Schuur, E. A. G., McGuire, A. D., Schadel, C., Grosse, G., Harden, J. W., Hayes, D. J.,
818   Hugelius, G., Koven, C. D., Kuhry, P., Lawrence, D. M., Natali, S. M., Olefeldt, D.,
819   Romanovsky, V. E., Schaefer, K., Turetsky, M. R., Treat, C. C., and Vonk, J. E.: Climate
820   change and the permafrost carbon feedback, Nature, 520, 171–179,
821   https://doi.org/10.1038/nature14338, 2015.

822 Soegaard, H. & Nordstroem, C.: Carbon dioxide exchange in a high-arctic fen estimated by eddy
823   covariance measurements and modeling, Glob. Change Biol., 5, 547–562,
824   https://doi.org/10.1111/j.1365-2486.1999.00250.x, 1999.

Strom, L., Tagesson, T., Mastepanov, M., and Christensen, T. R.: Presence of Eriophorum
      scheuchzeri enhances substrate availability and methane emission in an Arctic wetland,
      Soil Biol. Biochem., 45, 61–70, http://doi.org/10.1016/j.soilbio.2011.09.005, 2012.

Walker, D. A., Raynolds, M. K., Daniëls, F. J. A., Einarsson, E., Elvebakk, A., Gould, W. A.,
      Katenin, A. E., Kholod, S. S., Markon, C. J., Melnikov, E. S., Moskalenko, N. G., Talbot,
      S. S., Yurtsev, B. A. and the other members of the CAVM Team: The Circumpolar
      Arctic vegetation map, Journal of Vegetation Science, 16, 267-282,
      https://doi.org/10.1111/j.1654-1103.2005.tb02365.x, 2005.
Welker, J.M., Fahnestock, J.T., Henry, G.H.R., O'Dea, K.W. and Chimner, R.A.: CO_2 exchange
      in three Canadian High Arctic ecosystems: response to long-term experimental warming.
      Global Change Biology, 10, 1981-1995. Doi: 1011/j.1365-2486.2004.00857.x, 2004.

Vanderpuye, A. W., Elvebakk, A. and Nilsen, L.: Plant communities along environmental
      gradients of high-arctic mires in Sassendalen, Svalbard, J. Veg. Sci., 13, 875–884,
      http://doi.org/ 10.1111/j.1654-1103.2002.tb02117.x, 2002.

Vickers, H., Karlsen, S. R. and Malnes, E.: A 20-Year MODIS-Based Snow Cover Dataset for
      Svalbard and Its Link to Phenological Timing and Sea Ice Variability, Remote Sens., 12,
      1123; doi:10.3390/rs12071123, 2020.

Wutzler, T., Lucas-Moffat, A., Migliavacca, M., Knauer, J., Sickel, K., Šigut, L., Menzer, O. and
      Reichstein, M.: Basic and extensible post-processing of eddy covariance flux data with
      REddyProc, Biogeosciences, 15(16), 5015-5030, Doi:10.5194/bg-15-5015-2018, 2018.

Zhang, W., Jansson, P-E., Sigsgaard, C., McConnella, A., Jammet, M.M., Westergaard-Nielsen,
      A., Lund, M., Friborg, T., Michelsen, A., and Elberling, B.: Model-data fusion to assess
      year-round CO2 fluxes for an arctic heath ecosystem in West Greenland (69°N),
      Agricultural and Forest Meteorology, 272-273, 176-186,
      https://doi.org/10.1016/j.agrformet.2019.02.021, 2019.